

Micro-Quantification of Helium-3 and Helium-4 in TPBAR Components

February 2024

- 1 - Christopher DeFelice
- 2 - Martin Liezers
- 3 - Dallin Barton
- 4 - Connor Hilton

DISCLAIMER

This report was prepared as an account of work sponsored by an agency of the United States Government. Neither the United States Government nor any agency thereof, nor Battelle Memorial Institute, nor any of their employees, makes **any warranty, express or implied, or assumes any legal liability or responsibility for the accuracy, completeness, or usefulness of any information, apparatus, product, or process disclosed, or represents that its use would not infringe privately owned rights.** Reference herein to any specific commercial product, process, or service by trade name, trademark, manufacturer, or otherwise does not necessarily constitute or imply its endorsement, recommendation, or favoring by the United States Government or any agency thereof, or Battelle Memorial Institute. The views and opinions of authors expressed herein do not necessarily state or reflect those of the United States Government or any agency thereof.

PACIFIC NORTHWEST NATIONAL LABORATORY
operated by
BATTELLE
for the
UNITED STATES DEPARTMENT OF ENERGY
under Contract DE-AC05-76RL01830

Printed in the United States of America

Available to DOE and DOE contractors from
the Office of Scientific and Technical Information,
P.O. Box 62, Oak Ridge, TN 37831-0062

www.osti.gov

ph: (865) 576-8401

fox: (865) 576-5728

email: reports@osti.gov

Available to the public from the National Technical Information Service
5301 Shawnee Rd., Alexandria, VA 22312

ph: (800) 553-NTIS (6847)

or (703) 605-6000

email: info@ntis.gov

Online ordering: <http://www.ntis.gov>

Micro-Quantification of Helium-3 and Helium-4 in TPBAR Components

February 2024

1 - Christopher DeFelice
2 - Martin Liezers
3 - Dallin Barton
4 - Connor Hilton

Prepared for
the U.S. Department of Energy
under Contract DE-AC05-76RL01830

Pacific Northwest National Laboratory
Richland, Washington 99354

Abstract

This report documents the method development for measuring helium isotopes in micrometer-sized samples of tritium producing burnable absorption rod (TPBAR) components. Helium isotopes were measured as a tracer for tritium, which decays to ^3He with a half-life of 12.33 years. Getter and cladding materials from the TPBARs were analyzed as they are designed to restrict the movement of tritium. Therefore, constraining the diffusivity of tritium through these materials is of key importance. To first establish the reliability of the noble gas mass spectrometer, a reference gas with a relative $^4\text{He}/^3\text{He}$ ratio of ~ 1000 was pre-mixed. This standard was measured several times to ensure measurements were reproducible. Unirradiated and irradiated getter and cladding samples of TPBARs were cut into $1\text{-}100\ \mu\text{m}^3$ cubes and analyzed for ^3He and ^4He content. The unirradiated materials had helium content below the instrument's detection limit. Irradiated cladding also had levels of helium below the instrument's detection limit while irradiated getters had measurable levels of ^3He , interpreted to be the decay product of tritium. These findings validate this method as a way to trace tritium diffusion in reactor materials. To also measure ^4He with this method, larger sample sizes would be required. However, for irradiated samples, these sample sizes would likely not be volumetrically-releasable for tritium content.

Acknowledgments

The authors would like to thank the Tritium Technology Program for funding this project. The authors would also like to thank Michael Rodriguez and Richard Cox for providing a helium reference gas, Dallas Reilly for support with the SEM-FIB, Bethany Matthews and Randall Storms for providing access to samples, and David Senior, Andy Casella, and Josh Silverstein for their thoughtful questions and guidance throughout the project.

Acronyms and Abbreviations

a – anum
Al – Aluminum
Amu – atomic mass unit
 β - Beta
C – Carbon
CH₄ – Methane
Cm - centimeter
CO₂ – Carbon dioxide
CPS – counts per second
D – Deuterium
g – grams
Ga- gallium
H – Hydrogen
He – Helium
IC – Ion counter
kV – Kilovolt
Li – Lithium
mm – millimeter
Mo – Molybdenum
m/z – mass to charge ratio
N₂ – Nitrogen
nA - nanoampere
NG-MS – Noble gas mass spectrometer
O - Oxygen
O₂ – Oxygen
pg - picogram
PNNL – Pacific Northwest National Laboratory
Pt - Platinum
PWR – Pressurized water reactor
RPL – Radiochemical Processing Laboratory
SD – Standard deviation
SE – Standard error
SEM-FIB – Scanning electron microscope with focused ion beam
SNF – Spent nuclear fuel
TEM – Transmission electron microscope
TPBAR – Tritium producing burnable absorption rod
t_{1/2} – Half-life

Contents

Abstract.....	ii
Acknowledgments.....	iii
Acronyms and Abbreviations.....	iv
1.0 Introduction	1
1.1 Background.....	1
1.2 Overview of Problem.....	1
1.3 Project Goal	2
2.0 Materials and Methods	3
2.1 Samples.....	3
2.2 SEM-FIB	3
2.3 Noble Gas Mass Spectrometry	4
2.3.1 Method Overview.....	4
2.3.2 Isobaric Interferences	6
3.0 Results	9
4.0 Discussion.....	11
5.0 Future Directions	13
6.0 Conclusion	14
7.0 References.....	15

Figures

Figure 1. Sample preparation method via FIB lift-out technique. (a) trenches milled on either side (b) Easylift (TFS) tungsten-based needle brazed to the bar with the sides and bottom cut out so that it is attached now only to the needle. (c) Section of the attached bar to the Mo grid and cut away. Three views of a 1 μm^3 bar including (d) front, (e) side, and (f) back shown. All images shown are 52° in relationship to the imaging beam (0° would be top view and 90° would be direct side-view observation).....	4
Figure 2. Sample preparation bench (A) and Noblesse Noble Gas Mass spectrometer (B).....	5
Figure 3. Results of repeated measurements of ^3He enriched reference gas produced at 325RPL. The dashed line represents the average measured value, and the bold grey lines above and below the data is the two-standard deviation of all measurements.....	6
Figure 4. Mass scan across the ^3He and hydride peaks. The lower mass peak is $^3\text{He}^+$, while the higher mass peak are the hydrides (DH^+). The valley that can be seen between the two peaks indicate the mass resolution is sufficient to resolve this interference.....	7

Figure 5. Mass scan across the ^4He peak. Labels indicate the relative position of the $^{12}\text{C}^{3+}$ peak, the combined $^{12}\text{C}^{3+}$ peak, and the ^4He peak.....8

Figure 6. Measured CPS of irradiated (filled symbols) and unirradiated (hollow symbols) samples for both (A) ^3He and (B) ^4He . Note that (A) uses a log scale for the y-axis to show all data. Thick black line represents the average laser cell blank level over the analytical sessions, with the standard deviation being smaller than the thickness of the line. The dashed black line represents the instrument’s detection limit.9

Tables

Table 1. Descriptions and identifiers for the getter and cladding samples used in this study.....3

Table 2. $^4\text{He}/^3\text{He}$ ratio data for a mixed helium reference gas produced in 325RPL at PNNL.....6

Table 3. Raw CPS for analyzed samples in this study.....10

1.0 Introduction

1.1 Background

Helium is a noble gas that has a concentration of 5.22-5.24 ppm in the atmosphere (Oliver et al., 1984). Helium has two isotopes, ^4He and ^3He , and over 99.9998% of naturally occurring helium is ^4He . Helium-4 in the atmosphere is a product of thorium and uranium decay in the Earth's crust (Kockarts, 1973). Helium-3 on Earth is naturally generated in the upper atmosphere caused by nitrogen interacting with cosmic rays to produce ^3H , which then decays to ^3He (Libby 1946; Fireman, 1953), or by cosmic rays interacting with crustal lithium (Aldrich and Nier, 1948). Some ^3He also remains from the formation of the Earth (Craig and Lupton, 1976). This leads to a quite extreme, naturally occurring ratio of $^3\text{He}/^4\text{He}$ ratio of $\sim 1.4 \times 10^{-6}$ (Mamyrin and Tolstikhin, 2013). This ratio often makes ^3He an attractive isotopic tracer, as minute changes to its abundance will drastically change the $^3\text{He}/^4\text{He}$ ratio. It has been used historically to trace an un-degassed, primordial reservoir of material deep in the Earth (Craig and Lupton, 1976) and decay of ^3H in the environment (Kaufman and Libby, 1954).

Tritium is a rare, naturally occurring radionuclide. It can be found in the environment either as a gas (HT) or as a liquid (HTO). It is primarily produced by a reaction between cosmic rays and nitrogen in the upper atmosphere (Libby, 1946; Fireman, 1953) or as a rare decay product of thorium and uranium in Earth's crust, which has a negligible contribution to the total amount of ^3H (Kaufman and Libby, 1954). Overall, the total amount of tritium produced these ways is extremely low, accounting for less than one ^3H atom per 10^{18} hydrogen atoms (Kaufman and Libby, 1954). Large amounts of tritium were injected into the atmosphere during nuclear weapons testing between the 1940s until 1980, but due to its short half-life, background tritium levels have returned to pre-testing levels (Rozanski et al., 1991; van Rooyan et al., 2021). Tritium is produced in larger quantities anthropogenically during irradiation of certain materials. This is accomplished by the bombardment of ^6Li with neutrons, producing ^4He and ^3H . It can also be produced in the reactor when boron control rods are irradiated (Phillips and Easterly, 1980), when boron-10 accepts a neutron and produces two ^4He atoms and one ^3H atom. One ^3H is also produced per 10,000 fissions of uranium-235 or plutonium-239. Tritium is a radiogenic nuclide that decays to ^3He via beta emission with a short half-life of 12.33 a (Alvarez and Cornog, 1939, Oliver et al., 1987). As previously established, ^3He is an incredibly rare, stable, and low abundance isotope of helium. This makes ^3He an attractive target isotope to trace tritium.

Tritium is an important resource to support the United States' nuclear program. Tritium producing burnable absorption rods (TPBARs) are designed to be used in pressurized water reactors (PWR) with the purpose of producing tritium. At the center of a TPBAR is a LiAlO_2 pellet, which absorbs neutrons and ^6Li is converted to ^3H via neutron activation. The pellet is wrapped in a nickel-plated Zircaloy-4 jacket, called a getter, which captures ^3H . Outside of the getter is an aluminide-coated wrapping, called cladding, made of stainless steel to further mitigate any ^3H from diffusing out of the TPBAR.

1.2 Overview of Problem

It is key to understand the performance of the getter and cladding within a TPBAR in order to limit activation and fission products (e.g., tritium) from contaminating the reactor coolant system and potentially escaping to the environment (e.g., Suman et al., 2015). However, the direct observation and experimental work to verify the efficacy of cladding and getter material post-

irradiation is difficult due to radiological health and safety concerns for analysts and contamination concerns for the instruments used to measure the material. Measuring tritium in these materials is further complicated by the fact that tritium is a hard to detect radionuclide with a weak beta (β) emission. Additionally, it can take years to perform post irradiation examinations of irradiated TPBARs. This includes reanalyzing old samples using new analytical techniques to answer new questions. The relatively short half-life of tritium can make detecting ^3H in reactor materials after significant decay challenging (Bruno et al., 2020). A microanalysis technique capable of overcoming these challenges and allowing the investigation of how tritium diffuses through the various materials present in TPBARs is needed.

1.3 Project Goal

The goal of this project is to determine whether it is possible to detect ^3He and ^4He in micron-sized TPBAR components. We use ^3He as an analog for ^3H to overcome the challenges with its hard-to-detect nature and short half-life. Micron-sized samples are investigated in order to demonstrate the feasibility of observing tritium diffusion at a high spatial resolution, such as the thickness of the aluminide-coating on cladding. Furthermore, micron-sized samples provide the additional benefit of minimizing the activity of the irradiated materials to a level below concern for operator safety and instrument contamination.

2.0 Materials and Methods

2.1 Samples

Based on their design and purpose, the nickel-plated Zircaloy-4 getter and the aluminide-coated Zircaloy-4 cladding were selected for this study. Even though ^3He is a rare isotope, it is important to establish a baseline, or background, signal for this isotope. To do so, unirradiated samples of TPBAR getter and cladding were selected to measure this baseline of helium that may be inherent to the samples. Irradiated samples of TPBAR getter and cladding were selected for analysis as having the highest likelihood of capturing ^3H , which would lead to radiogenic ingrowth of ^3He . Details of the samples selected are in Table 1.

Table 1. Descriptions and identifiers for the getter and cladding samples used in this study.

	Getter Sample	Cladding Sample
Unirradiated	Piece of FLG, Hohman Lot # 98667-111026, Veridiam Lot # 23017-0001 Remnants from Trit-M-TRV-015	Production Coated Cladding Tube from Wesdyne WDI-NDP-15-167 Rev 1, MB-24-P260 Drawing & Rev H-3-307847 REv8 Remarks Tube 6801-0046-245
Irradiated	GC13-2-3-2-FLG26	C13-2-3-2(CLAD26)

2.2 SEM-FIB

The samples (both with and without irradiation) were created using a Helio Nanolab 660 (Thermo Fisher Scientific, TFS) dual Ga-based focused ion beam/scanning electron microscope (FIB/SEM). The SEM-FIB is located in the 325 Radiochemical Processing Laboratory (325RPL) at the Pacific Northwest National Laboratory (PNNL). Samples were created via the “lift-out” method commonly used for other nano-scale analysis such as transmission electron microscopy or atom probe tomography (Barton et al., 2021; Das et al., 2023). Samples were milled out of the midpoint of the thickness of the material. Trenches were cut parallel to the ion beam on two sides of the sample at an accelerating voltage of 30 kV and a current of 9 nA and then tilted 52° from the direction of the ion beam (Figure 1a) for cutting underneath the sample and the side of the sample at a current of 3 nA. The resulting cantilever was brazed to a tungsten needle (TFS Easylift) using Pt via the gas infiltration system (Figure 1b). The final connecting piece was cut free and the small sample was removed from the bulk of the material. The sample was then brazed to a Mo coupon holder often used for TEM (Omniprobe Lift-out grid). The coupon is a 3 mm diameter half-circle mounting posts coming out of the half circle (Figure 1c). Each sample was attached to individual coupons. Sample volumes for the non-radiological materials were nominally 1 μm^3 , 10 μm^3 , and 100 μm^3 . Sample volumes for the irradiated cladding materials were also 1 μm^3 , 10 μm^3 , and 100 μm^3 . Due to the estimated radiological material in the getter material, only 1 μm^3 volumes were created.

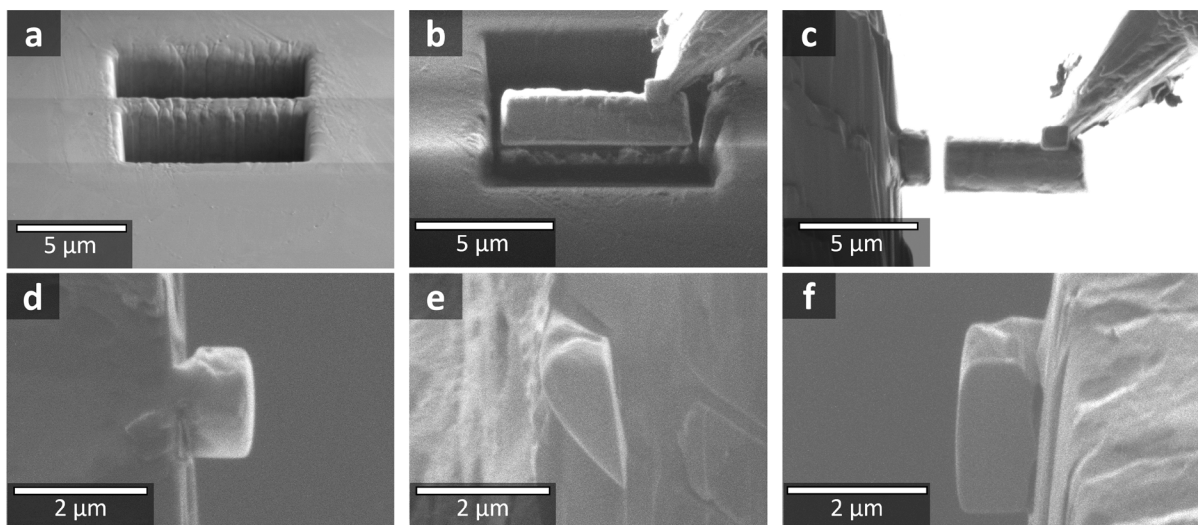


Figure 1. Sample preparation method via FIB lift-out technique. (a) trenches milled on either side (b) Easylift (TFS) tungsten-based needle brazed to the bar with the sides and bottom cut out so that it is attached now only to the needle. (c) Section of the attached bar to the Mo grid and cut away. Three views of a $1 \mu\text{m}^3$ bar including (d) front, (e) side, and (f) back shown. All images shown are 52° in relationship to the imaging beam (0° would be top view and 90° would be direct side-view observation).

2.3 Noble Gas Mass Spectrometry

2.3.1 Method Overview

Noble gases can be difficult to directly measure due to being chemically inert and their high ionization energies. Generally, mass spectrometers all have the same three basic components: an ion source, which ionizes elements of interest by stripping away electrons to convert them to cations with a +1 charge, a mass filter, such as an electromagnet to bend the ion's path based on its mass, and detectors, used to measure the strength of the ion's signal. Mass spectrometers typically measure the mass to charge ratio (m/z) of elements. The Noblesse Noble Gas Mass Spectrometer (NG-MS) is specifically designed to ionize and measure noble gases with a Nier-type source, electromagnet mass filter, and ion counters (IC) which can measure low abundance signals. This makes the Noblesse NG-MS ideal for measuring noble gases, such as helium.

During the duration of this project, the power supply of the mass spectrometer, which is used to power the ion source which ionizes the sample gas so it can be measured by the detectors, was unstable. While measurements during a single analytical session would be consistent, day-to-day measurements could vary. The unstable power led to the ionization filament having to be replaced several times during the project, which also contributes to short-term variability in measurements.

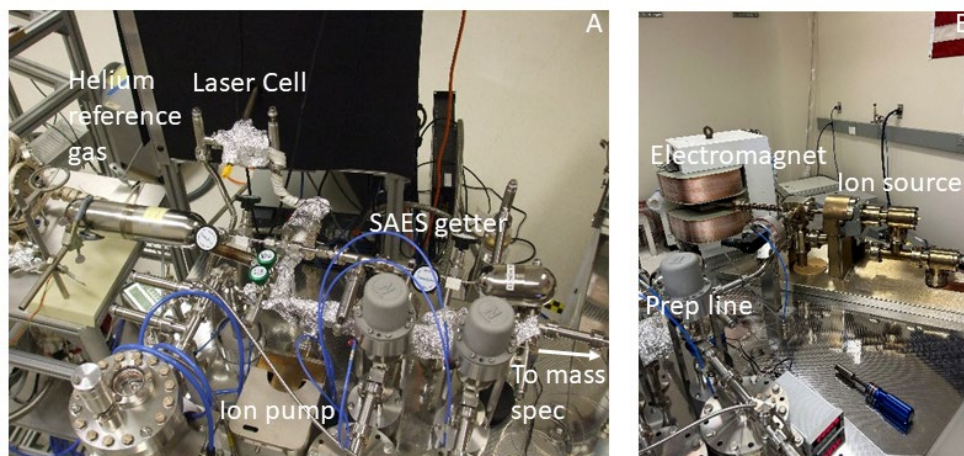


Figure 2. Sample preparation bench (A) and Noblesse Noble Gas Mass spectrometer (B).

Samples on Mo grids were loaded into a Fusions CO₂ laser system (Teledyne Photon Machines, Omaha, NE, USA). The laser cell is connected to a preparation line for the NG-MS, making the analysis of solid samples possible (Figure 2). Gas was released from samples by heating the Mo grid. Blank samples, which were unirradiated getter and cladding materials, were also measured for their helium content to make sure any ³He measured in the irradiated samples is a daughter product of tritium and not naturally found in the material. The laser was focused on the center of the Mo grid and fired at 50% power (15 watts) with a spot size of 1 mm for 5 seconds. By heating the grid, the gas is driven out of the mounted sample and into the Noblesse preparation line where it interacts with a SAES GP50 getter for 600 seconds to remove any reactive gases (O₂, N₂, CH₄) before being introduced to the mass spectrometer. The NG-MS was operated in static mode, where a finite amount of gas is let into the mass spectrometer for analysis. Laser blanks and unirradiated samples were measured using an ion counter (IC) using peak hopping, where an off-peak ³He and ⁴He 'zero' is taken half an atomic mass unit off the measured peaks. Then both masses of helium are measured sequentially. A peak centering routine was done before each analysis using a reference gas, which was mixed in 325RPL with an estimated ⁴He/³He = 1000. This estimate was based on pressure readings while mixing the ³He and ⁴He gas sources. As such, this reference gas was used to test the reproducibility of the measurements but could not be used to assess measurement accuracy.

The results of seven analyses of the reference gas are shown in Figure 3 and ⁴He/³He ratios are given in Table 2. To make this measurement, the same amount of gas was introduced to the mass spectrometer and masses 4 and 3 were measured sequentially. Due to the sensitivity of the ion counter, and the significantly larger amount of ⁴He to ³He, a target signal of ~1000 counts per second or less was set for ³He. This was done to limit the signal observed on the ⁴He beam, which if too large, could damage the ion counter detector. The average measured ⁴He/³He ratio was $\sim 1230 \pm 80$ (2*standard deviation), which is in broad agreement with the expected ratio of the reference gas (~1000).

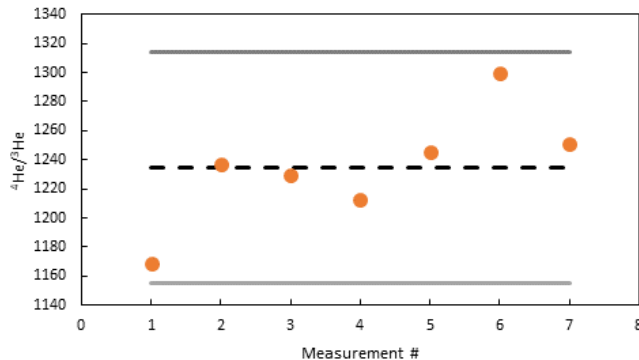


Figure 3. Results of repeated measurements of ^3He enriched reference gas produced at 325RPL. The dashed line represents the average measured value, and the bold grey lines above and below the data is the two-standard deviation of all measurements.

Table 2. $^4\text{He}/^3\text{He}$ ratio data for a mixed helium reference gas produced in 325RPL at PNNL.

Measurement	$^4\text{He}/^3\text{He}$	Standard Error
1	1168.88	240
2	1236.81	6.60
3	1229.04	13.0
4	1213.12	13.0
5	1245.34	13.0
6	1299.50	6.70
7	1250.80	14.0
Average	1234.78	
2 SD	79.19	

SD = Standard deviation

2.3.2 Isobaric Interferences

Both ^3He and ^4He suffer from isobaric interferences, which are elements or molecules that have very similar or overlapping atomic masses. This provides an analytical challenge to separate the isotopes of interest from other isotopes/molecules sharing a similar atomic mass. It is important to determine which signals are from other elements/molecules that need to be avoided during measurement. For ^3He , the near-by hydrogen-deuterium (HD^+) needs to be avoided (Hooker et al., 1985; Schwanethal, 2015). This peak can often have a much stronger signal than ^3He due to the generally larger abundances of hydrogen in nature over helium and can be difficult to avoid. A mass spectrometer with sufficient mass resolution, or the ability to separate out signals of different isotopes/molecules, is required. The Noblesse NG-MS has a mass resolution of at least 750 (defined as the peak of the mass interest being observed divided by the width at half

the peak height) which is sufficient to resolve this interference (Schwanethal, 2015). This allows the direct measurement of ^3He by carefully selecting the correct mass (Figure 4). Even with a mass resolution that can separate hydrides from ^3He , it is possible the mass spectrometer may select the wrong signal due to their closeness. To avoid that and ensure ^3He was being measured, an offset value was applied to the measurement routine where the high-mass shoulder was identified and then the magnet set point was shifted by 0.002 amu towards the low-mass side to ensure the correct peak was measured (Figure 4).

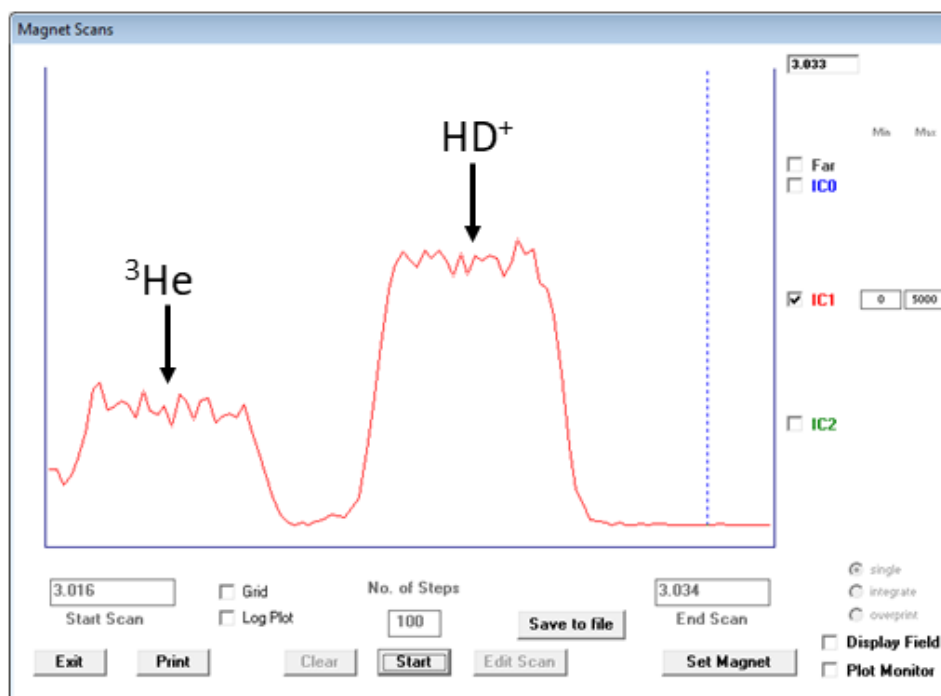


Figure 4. Mass scan across the ^3He and hydride peaks. The lower mass peak is $^3\text{He}^+$, while the higher mass peak are the hydrides (DH^+). The valley that can be seen between the two peaks indicate the mass resolution is sufficient to resolve this interference.

Helium-4 has a more difficult interference with $^{12}\text{C}^{3+}$ ($m/z = 4$) that cannot be resolved (Schwanethal, 2015). The interference is more obvious at low signals (Figure 5) and difficult to observe at larger signals. This isobaric interference makes it difficult to directly measure ^4He , as the overlying $^{12}\text{C}^{3+}$ signal creates a complex peak shape. Unlike the ^3He peak, which has sharp, tall sides and a relatively flat peak-top, the ^4He peak shape has two shoulders of differing intensities and a sloped peak top. This is caused by the overlying $^{12}\text{C}^{3+}$ isobaric interference. To properly measure ^4He , it is important to identify which isotopes are contributing to the peak. In the middle of the peak is the combined signal of $^{12}\text{C}^{3+}$ and ^4He . Based on their calculated masses, the high mass shoulder is the helium peak, which has a slightly lower intensity than the peak top, leading to the overall sloped peak-top. There are two approaches to properly measuring ^4He – measuring the combined ^4He and $^{12}\text{C}^{3+}$ peak or using an offset value to measure only the ^4He peak – where the magnet is set to a mass value on the shoulder of the peak, and then moved by a predefined value, similar to how ^3He is measured. The approach taken in this project is to use an offset value, as the Noblesse has the mass resolution to clearly see the ^4He high mass shoulder. This method is additionally validated by measuring a correct $^4\text{He}/^3\text{He}$ ratio in the 325RPL mixed reference gas (Figure 3).

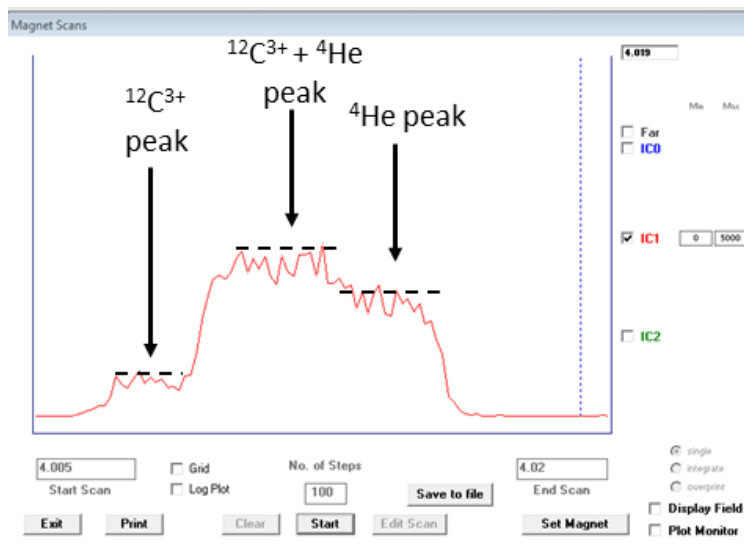


Figure 5. Mass scan across the ${}^4\text{He}$ peak. Labels indicate the relative position of the ${}^{12}\text{C}^{3+}$ peak, the combined ${}^{12}\text{C}^{3+}$ peak, and the ${}^4\text{He}$ peak.

3.0 Results

The average counts per second (CPS) of ^4He and ^3He from the blank laser cell measurements, the measurements of unirradiated samples, and measurements of irradiated samples are presented in Figure 6 and listed in Table 3. The detection limit for ^4He and ^3He for the mass spectrometer was calculated as $9.925 \times \text{SD}$ of the four blank laser cell measurements. These resulted in detection limits of 56,000 cps and 71 cps, respectively. For all samples, the ^4He signal observed was less than the detection limit. The ^3He signal observed was also below the detection limit for most samples. Only the irradiated getter samples contained detectable ^3He . Of the three $1 \mu\text{m}^3$ irradiated getter samples, the first sample was measured twice, corresponding to two separate laser heating events, to ensure all gas from the sample was released.

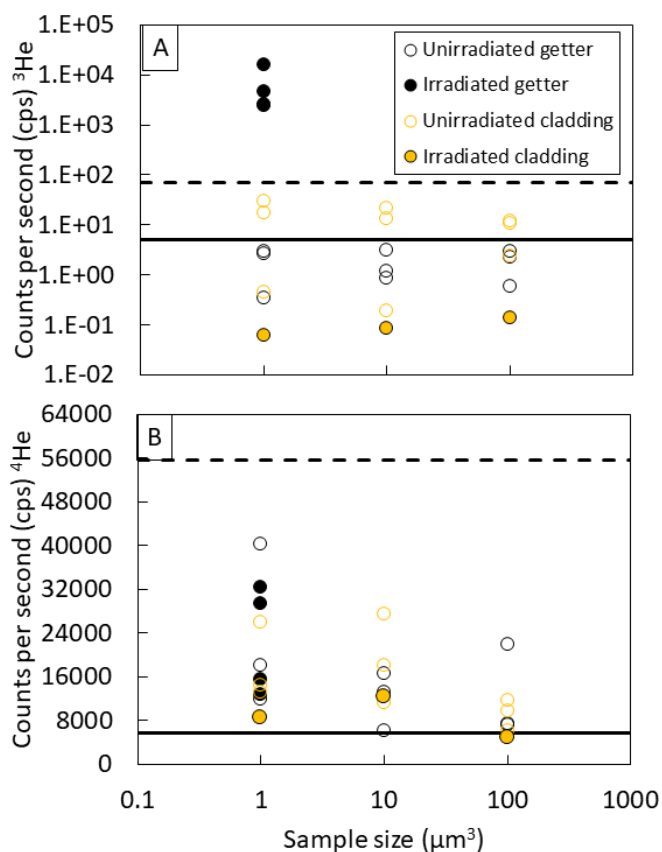


Figure 6. Measured CPS of irradiated (filled symbols) and unirradiated (hollow symbols) samples for both (A) ^3He and (B) ^4He . Note that (A) uses a log scale for the y-axis to show all data. Thick black line represents the average laser cell blank level over the analytical sessions, with the standard deviation being smaller than the thickness of the line. The dashed black line represents the instrument's detection limit.

Table 3. Raw CPS for analyzed samples in this study.

Sample	Irradiated or unirradiated*	Sample size (μm^3)	^4He (cps)	SE	^3He (cps)	SE
Getter	U	1	40,200	300	0.3	0.2
Getter	U	1	18,100	100	2.9	0.3
Getter	U	1	11,900	100	2.7	0.3
Cladding	U	1	14,400	200	0.5	0.2
Cladding	U	1	25,970	50	29.4	0.7
Cladding	U	1	13,140	40	17.2	0.4
Getter	U	10	16,500	200	0.9	0.2
Getter	U	10	6,070	40	3.1	0.2
Getter	U	10	13,100	100	1.2	0.5
Cladding	U	10	27,000	1,000	0.2	0.2
Cladding	U	10	18,000	1,000	21.8	0.6
Cladding	U	10	11,220	30	13.5	0.5
Getter	U	100	21,900	60	0.6	0.2
Getter	U	100	7,150	70	2.9	0.2
Getter	U	100	7,320	80	2.2	0.2
Cladding	U	100	11,600	200	2.4	0.5
Cladding	U	100	6,150	50	11	2
Cladding	U	100	9,700	100	12.1	0.5
Getter	I	1	29,310	60	4,660	10
Getter ^a	I	1	32,310	70	15,990	40
Getter	I	1	15,510	50	2,430	10
Getter	I	1	12,700	100	2,590	20
Cladding	I	1.	8,510	30	0.06	0.04
Cladding	I	10	12,410	40	0.08	0.08
Cladding	I	100	4,800	30	0.1	0.1
Laser cell blank average and SD ^b			4,600	5,600	5.2	7.2
Detection Limit ^c			56,000		71	

*I = irradiated sample, U = unirradiated sample.

SE = Standard error of the measurement.

SD = Standard deviation of the measurements.

(a) = Second measurement of above sample after additional heating.

(b) = Laser cell blank is the average of 4 measurements taken on days where data were collected.

(c) = Detection limit defined as $9.925 \times \text{SD}$ of the laser cell blank measurements.

4.0 Discussion

All samples analyzed in this study contained quantities of ^4He that were below the detection limit of the mass spectrometer. Similarly, the quantities of ^3He were below the instrument's detection limit for the unirradiated cladding and getter samples as well as the irradiated cladding samples. As such, no conclusions can be drawn about the relative He content of these materials or the behavior of He or tritium diffusivity. The $1\ \mu\text{m}^3$ irradiated getter samples did contain several thousand CPS of ^3He , however. The presence of this isotope is most certainly from the decay of tritium, given the lack of detectable ^3He in the other samples. This makes sense, as the getter is designed to trap tritium. After some period of time, ^3He would ingrow.

The average $^4\text{He}/^3\text{He}$ ratio of the irradiated C13 getters is reported to be 0.04 ± 0.08 . If this ratio is assumed for the $^4\text{He}/^3\text{He}$ ratio of the $1\ \mu\text{m}^3$ irradiated getter samples then the ^4He signal present in these samples would be between 100 and 700 cps, based on the measured ^3He signal. Since the ^4He detection limit was 56,000 cps, it is not surprising that ^4He was not detected in these samples. Since the $1\ \mu\text{m}^3$ irradiated getter samples were the largest sized samples that could be volumetrically-released for tritium contamination controls, it is not likely that the sample sizes for this method could be scaled up to provide measurable ^4He without changing the radiological controls of the Noblesse mass spectrometer.

While these data are below the instrument's detection limit, there is a general increasing signal of ^4He towards smaller sample sizes in both irradiated and unirradiated material. Additionally, for the one irradiated getter sample that was heated by the laser twice, more ^3He was observed in the second heating attempt than the first heating attempt. While not conclusive, these observations suggest that gas release by laser heating is dependent on the sample volume, with gas being more easily released from smaller volumes of material. Multiple heating episodes may need to be conducted in the future to ensure all gas is extracted from a sample.

While we do not know the exact age and ^3H loading level of the getter sample, it is possible to make some rough estimates of noble gas detection efficiency. The density of a typical non-evaporable hydrogen getter like ST707 (SAES Getters) is about $6\ \text{g cm}^3$ (Feng et al., 2018) which would yield a $1\ \mu\text{m}^3$ particle weight of $6 \times 10^{-12}\ \text{g}$. The maximum $^1\text{H}_2$ loading of this getter material has been reported as $8.14 \times 10^{-3}\ \text{moles g}^{-1}$ (Hsu and Millis, 2010). A $1\ \mu\text{m}^3$ particle could therefore hold up to 4.95×10^{-14} moles of $^1\text{H}_2$ or 2.98×10^{10} molecules of $^1\text{H}_2$. Assuming a moderate loading of 10% maximum capacity, this would make 2.98×10^9 molecules of $^3\text{H}_2$ potentially available in the irradiated $1\ \mu\text{m}^3$ getter cubes. The FIB cutting process will lightly release some hydrogen and helium due to heating, although most of the hydrogen species present will be chemically bound in the getter. For ^3He , losses are likely to be more significant as these atoms will not be chemically bound. Helium usually displays the lowest solubility and highest mobility of all the noble gases in most materials. Despite these factors, measurements on the Noblesse still yielded large ^3He signals from the irradiated getter samples. Significant variation in ^3He signal intensity was observed between the three $1\ \mu\text{m}^3$ particles, however. These differences might simply reflect slight variations in sample size or gas released through laser heating but they could also reflect sampling variations between the different metallic phases present in the getter or microscopic internal sample voids that formed during the hydrogen absorption process. Larger specimens may homogenize these microscopic effects and reduce variation in ^3He observed between samples.

If we use a 6 year decay period then about 25% of the available tritium atoms would have decayed. This would yield about 1.49×10^9 ^3He atoms available in a $1\ \mu\text{m}^3$ getter sample, ignoring the losses from the FIB cutting process. Based on the ^3He count rates observed for the

3 getter samples (1 = 15985 cps, 2 = 2431 cps, 3 = 2587 cps) this would yield a detection efficiency in the range 0.00016 – 0.0011%. Noble gas mass spectrometry can potentially achieve a detection efficiency of ~0.1% for xenon, but He displays lower sensitivity due to its higher ionization potential, and the gas loss caused by the sample preparation process was ignored. The detection efficiency therefore seems reasonable and can likely be improved.

5.0 Future Directions

This study has shown it is possible to measure ^3He derived from tritium decay in micronmeter sized TPBAR components to trace tritium diffusion. It is interpreted that the measured ^3He in the irradiated getter sample is the daughter product of tritium, due to the extremely low naturally occurring abundance and low background of ^3He observed in all the unirradiated samples tested. Based on these findings, several avenues of future work can be explored using this method.

It is possible to quantify the amount of helium measured. Currently, this is not possible with the NG-MS. However, it is possible to quantify the amount of helium using a spiked reference gas. This would involve acquiring a pipette of helium gas with a precisely known amount of both isotopes of helium. Based on the measured amount of ^3He , the decay constant of tritium, age since irradiation, and the estimated sample size, it would be possible to calculate the starting concentration of tritium in a sample. This could be used to estimate how much tritium is being adsorbed by various reactor components.

While this report focuses on whether or not ^3He is detectable in cladding and getter material at the micron scale, it is possible to measure the $^4\text{He}/^3\text{He}$ ratio of materials using this method. However, given the ^4He content of these samples relative to the instrument's detection limit, larger sample sizes would be required. Sensitivity to ^4He could be improved by minimizing the interference from $^{12}\text{C}^{3+}$. This has already been investigated by Schwanethal (2015) by altering some of the tuning parameters on the source of the NG-MS, such as the trap voltage. This work could be expanded on, and replicating their method could be beneficial, especially if there is interest in the $^4\text{He}/^3\text{He}$ ratios of materials or quantifying the amount of ^4He gas.

There are other parts of the reactor that may be exposed to tritium. The NG-MS is a versatile instrument that can analyze samples of different compositions, such as liquids. This method could be applied to many parts of the reactor to find ^3He as a tracer of tritium and, unlike β counting methods, it is blind to the presence of other radioisotopes.

6.0 Conclusion

This report documents a new method for tracing ^3H through its daughter product ^3He . Getter and cladding material from TPBARs were selected for testing, as they are designed to capture and prevent the loss of activation and fission products from the TPBAR. The size of samples ranged from $1\ \mu\text{m}^3$ to $100\ \mu\text{m}^3$ to eliminate any radiation hazards during analysis. Unirradiated samples and irradiated cladding contained no measurable helium above the instrument's detection limits. Irradiated getter material of $1\ \mu\text{m}^3$ contained several thousand CPS of ^3He , corresponding to a total sample weight of 5-10 pg. Modern methods of detecting tritium require milligrams of sample (Torikai, 2021), meaning this method is several orders of magnitude more sensitive to tritium detection, albeit indirectly. Despite the heating process by the FIB to cut samples, ^3He was still detectable in the irradiated getter samples. This is an interesting result, as the He in the material exists as a gas and is not chemically attached to the getter, unlike tritium. This suggests that sample sizes could be reduced further and still get measurable results for ^3He . The success of this method has opened several avenues of potential future work in the detection of tritium in TPBARs and nuclear reactors.

7.0 References

- Aldrich, Lyman Thomas, and Alfred O. Nier. "The occurrence of He 3 in natural sources of helium." *Physical Review* 74, no. 11 (1948): 1590.
- Alvarez, Luis W., and Robert Cornog. "Helium and hydrogen of mass 3." *Physical Review* 56, no. 6 (1939): 613.
- Barton, D.J., Hornbuckle, B.C., Darling, K.A., Brewer, L.N., Thompson, G.B. "Influence of surface temperature in the laser assisted cold spray deposition of sequential oxide dispersion strengthened layers: Microstructure and hardness." *Materials Science and Engineering. A* 811 (2021).
- Bruno, Jordi, Lara Duro, and François Diaz-Maurin. "Spent nuclear fuel and disposal." In *Advances in Nuclear Fuel Chemistry*, pp. 527-553. Woodhead Publishing, 2020.
- Craig, H., and J. E. Lupton. "Primordial neon, helium, and hydrogen in oceanic basalts." *Earth and Planetary Science Letters* 31, no. 3 (1976): 369-385.
- Das, D., Sanchez, F., Barton, D.J., Tan, S., Shutthanandan, V., Devaraj, A., Ramana, C.V. "Rationally Engineered Vertically Aligned β -Ga₂-xW_xO₃ Nanocomposites for Self-Biased Solar-Blind Ultraviolet Photodetectors with Ultrafast Response." *Advanced Materials Technologies* 8(15) (2023).
- Fireman, E. L. "Measurement of the (n, H 3) Cross Section in Nitrogen and Its Relationship to the Tritium Production in the Atmosphere." *Physical Review* 91, no. 4 (1953): 922.
- Feng, Tianyou, Yongjun Cheng, Lian Chen, Zhenhua Xi, Jianbing Zhu, and Yali Li. "Hydrogen adsorption characteristics of Zr₅₇V₃₆Fe₇ non-evaporable getters at low operating temperatures." *Vacuum* 154 (2018): 6-10.
- Hooker, P. J., R. Bertrami, S. Lombardi, R. K. O'Nions, and E. R. Oxburgh. "Helium-3 anomalies and crust-mantle interaction in Italy." *Geochimica et Cosmochimica Acta* 49, no. 12 (1985): 2505-2513.
- Hsu, Irving, and Bernice E. Mills. *Hydrogen capacity and absorption rate of the SAES St707 non-evaporable getter at various temperatures*. No. SAND2010-5402. Sandia National Laboratories (SNL), Albuquerque, NM, and Livermore, CA (United States), 2010.
- Kaufman, Sheldon, and W. F. Libby. "The natural distribution of tritium." *Physical Review* 93, no. 6 (1954): 1337.
- Kockarts, Gaston. "Helium in the terrestrial atmosphere." *Space Science Reviews* 14, no. 6 (1973): 723-757.
- Libby, Willard F. "Atmospheric helium three and radiocarbon from cosmic radiation." *Physical Review* 69, no. 11-12 (1946): 671.
- Mamyrin, Boris Aleksandrovich, and Igor' Nesterovich Tolstikhin. *Helium isotopes in nature*. Elsevier, 2013.

Oliver, B. M., Harry Farrar IV, and M. M. Bretscher. "Tritium half-life measured by helium-3 growth." *International Journal of Radiation Applications and Instrumentation. Part A. Applied Radiation and Isotopes* 38, no. 11 (1987): 959-965.

Oliver, B. M., James G. Bradley, and Harry Farrar IV. "Helium concentration in the Earth's lower atmosphere." *Geochimica et Cosmochimica Acta* 48, no. 9 (1984): 1759-1767.

Phillips, J. E., and C. E. Easterly. *Sources of tritium*. No. ORNL/TM-6402. Oak Ridge National Lab., TN (USA), 1980.

Suman, Siddharth, Mohd Kaleem Khan, Manabendra Pathak, R. N. Singh, and J. K. Chakravartty. "Hydrogen in Zircaloy: Mechanism and its impacts." *International Journal of Hydrogen Energy* 40, no. 17 (2015): 5976-5994.

Schwanethal, James. "Minimising $^{12}\text{C}^{3+}$ interference on $^4\text{He}^+$ measurements in a noble gas mass spectrometer." *Journal of Analytical Atomic Spectrometry* 30, no. 6 (2015): 1400-1404.

Torikai, Yuji, "Tritium retention in dust particles and divertor tiles of JET operated with the ITER-Like Wall." Poster presented at the 28th International Atomic Energy Association Fusion Energy Conference, virtual, May 14, 2021. <https://conferences.iaea.org/event/214/contributions/17656>

Pacific Northwest National Laboratory

902 Battelle Boulevard
P.O. Box 999
Richland, WA 99354

1-888-375-PNNL (7665)

www.pnnl.gov